

2-P(mix)

SEPARATION OVER A FLAT PLATE-WEDGE CONFIGURATIONS  
AT OCEANIC REYNOLDS NUMBERS

By

David R. Campbell

May 8, 1973

no no no  
(NASA-CR-131888) SEPARATION OVER A FLAT  
PLATE-WEDGE CONFIGURATION AT OCEANIC  
REYNOLDS NUMBERS (Notre Dame Univ.)  
32 p HC \$3.75

CSCL 20D

N73-22233

Unclas

G3/12 02416

Backup Document for AIAA Synoptic Scheduled  
for Publication in the Journal of Hydronautics, October 1973

Energy Conversion Research Laboratory  
Department of the Air Force  
Aerospace Research Laboratories(AFSC)  
Wright-Patterson Air Force Base, Ohio 45433

### SYNOPTIC BACKUP DOCUMENT

This document is made publicly available through the NASA scientific and technical information system as a service to readers of the corresponding "Synoptic" which is scheduled for publication in the following (checked) technical journal of the American Institute of Aeronautics and Astronautics.

- ☐ AIAA Journal
- ☐ Journal of Aircraft
- ☐ Journal of Spacecraft & Rockets
- ☒ Journal of Hydronautics , October 1973

A Synoptic is a brief journal article that presents the key results of an investigation in text, tabular, and graphical form. It is neither a long abstract nor a condensation of a full length paper, but is written by the authors with the specific purpose of presenting essential information in an easily assimilated manner. It is editorially and technically reviewed for publication just as is any manuscript submission. The author must, however, also submit a full backup paper to aid the editors and reviewers in their evaluation of the synoptic. The backup paper, which may be an original manuscript or a research report, is not required to conform to AIAA manuscript rules.

For the benefit of readers of the Synoptic who may wish to refer to this backup document, it is made available in this microfiche (or facsimile) form without editorial or makeup changes.

SEPARATION OVER A FLAT PLATE-WEDGE  
CONFIGURATION AT OCEANIC REYNOLDS NUMBERS

David R. Campbell\*

Aerospace Research Laboratories  
Wright-Patterson Air Force Base, Ohio

ABSTRACT

An experimental study of flow over a two-dimensional flat plate-wedge configuration is presented. The investigation encompasses a range of Reynolds numbers characteristic of conditions encountered by deep submersible oceanic vehicles. Flow separation, similar to that found on high speed aircraft control surfaces, is reported and discussed in light of the laminar or transitional nature of the separated shear layer. As discovered in previous high Mach number studies of plate-wedge or ramp configurations, the dependency of the size of the separated region on free stream Reynolds number is reversed for laminar and transitional types of flow separation.

---

\*Research Aerospace Engineer, Energy Conversion Research Laboratory.  
Research performed at the Aerospace Laboratory, University of Notre  
Dame, under NASA Fellowship

PRECEDING PAGE BLANK NOT FILMED

NOMENCLATURE

$C_p$  =  $(P - P_\infty) / q_\infty$ , Pressure coefficient

$x$  = Coordinate distance measured along the direction of the flat plate surface

$P$  = Static Pressure

$q$  = Dynamic Pressure

$Re$  = Reynolds number

Subscripts

$C$  = Corner

$R$  = Reattachment

$S$  = Separation

$\infty$  = Free stream value

Preceding page blank

## INTRODUCTION

In the design of hydrodynamic vehicles, knowledge of the likely occurrence of flow separation, and factors that influence it, is extremely valuable if not essential. The occurrence of boundary layer separation over the compression corner formed by the wing and control surface of a high speed vehicle has been well documented by various researchers over the past fifteen years. One of the earliest studies of this problem was that of Chapman, Kuehn, and Larson<sup>1,2</sup> in the mid-1950's. Subsequently others performed similar experiments with two-dimensional, three-dimensional, and axisymmetric shapes, over the full range of supersonic and hypersonic Mach numbers, analyzing effects of surface heating and cooling and hinge line suction as well as the usual investigation of Mach and Reynolds number effects. References 3 through 10 are but a very small sampling of this body of research.

To this author's knowledge, there has been no effort whatsoever to investigate the similar phenomenon that occurs at extremely low velocities. In the case of supersonic flow over a plate-wedge configuration, the entire local flow field experiences increasing pressure in the stream direction. In the region near the surface, this of course results in boundary layer separation ahead of the compression corner. In contrast, the analogous low speed situation gives rise to two opposing pressure tendencies. In the region away from the surface, yet within the zone of influence of the wedge, the fluid accelerates in the stream direction consistent with a favorable pressure gradient. Near the surface, the

1

pressure field is dominated by the decelerative effect of the wedge obstructing the normal flow path. Here the fluid experiences an adverse pressure gradient which if sufficiently strong, results in a corner separation bubble not unlike that of the much higher Mach number case.

In the design of deep submersible vehicles for scientific exploration as well as potential military applications, control surfaces and other vehicle components will be subject to this latter type of low speed flow separation. The intent of this paper is to present experimental results for a flat plate-wedge configuration at very low Reynolds numbers, typical of submersibles in a deep oceanic environment, and draw some comparisons with the flow separation phenomenon of much higher Mach and Reynolds numbers.

#### TEST FACILITIES

Two different test facilities were used in the low Reynolds number tests of the plate-wedge configuration. Ultra low Reynolds number tests were performed in a hydrodynamic tow tank facility. At moderately low Reynolds numbers, a specially modified low turbulence wind tunnel was used.

Figure 1 depicts the essential features of the tow tank facility. The tank is fabricated of 1/2 inch Plexiglas, measuring 6 feet long, 7 inches wide, and 8 3/4 inches deep. The tank was filled to a depth of 7 inches with distilled water to which aluminum powder was added to serve as tracer particles for flow visualization.

A motor driven cart, to which a camera and model supporting sting were attached, rode on two parallel tracks above the tank. The walls and floor of the tank were draped outside with black velvet material to eliminate extraneous light. A light source consisting of a bank of spot lights behind a 1/8 inch slit illuminated a thin layer of the suspended aluminum particles. Photographic data was obtained by traversing the cart over the length of the tank with a model attached to the sting, taking time lapse photographs of the aluminum particle traces.

Wind tunnel experiments were conducted in a low turbulence indraft subsonic wind tunnel equipped with kerosene smoke flow visualization equipment. A two-stage contraction ratio of 50:1 and anti-turbulence screening was very effective in producing laminar conditions in a 17" by 17" test section. A special modification was added to the wind tunnel for low Reynolds number testing. A screened "bleed" section was inserted downstream of the test section just before the impellor to reduce the tunnel free stream velocity below its normal minimum. With the mass bleed device, free stream dynamic pressure as low as 0.016 inches of water was obtained. Further description of the two experimental facilities is contained in reference 11.

#### MODELS AND INSTRUMENTATION

For use in the tow tank facility, 20° and 30° wedge models were fabricated of hardwood stock. Plexiglas side plates were

employed to reduce three-dimensional effects in the flow field (see Figure 2). The transparent side plates permitted the central portion of the flow field to be illuminated from the side of the tank while photographed from above. The surface of the models was painted black to enhance photographic contrast. The wedges were positioned on the flat plate portion of the model so as to leave a distance of 11 inches between the leading edge of the model and the beginning of the wedge. The span dimension was 3 inches.

Wind tunnel models of  $20^\circ$  and  $30^\circ$  wedges (Figure 3) were fabricated of aluminum. The flat portion of the model was of 1/16 inch steel. Surface finish consisted of 18 coats of hand-rubbed black lacquer, waxed, and then polished. Side plates, 3/8 inch thick, one of velvet covered plywood and one of Plexiglas, helped reduce three-dimensional effects. The velvet covering was black to enhance contrast of smoke photographs. The beginning of the wedge incline was positioned 7 inches from the plate leading edge. The model span was 9 inches. The wind tunnel models were instrumented with surface static pressure taps. Figure 4 contains a layout of pressure tap locations, both along the model centerline and spanwise at three stations, for determining the two-dimensionality of the wedge flow field. The pressure taps consisted of 0.05 inch OD hollow stainless tubing mounted flush with the surface of the model.



## EXPERIMENTAL RESULTS AND DISCUSSION

An initial effort was made to determine the two-dimensionality of the water tank and wind tunnel experiments. By the method of streak line photography, it was determined that the side plate boundary layers on the tow tank wedge model were approximately  $3/4$  inches thick at the beginning of the wedge itself. This implied that one might reasonably expect 1 to  $1\frac{1}{2}$  inches of the flow along the centerline to be somewhat two-dimensional in nature. In the case of the wind tunnel models, spanwise surface pressure distributions indicated that at least 6 inches along the centerline was essentially two-dimensional.

With these two experimental set-ups, two ranges of test Reynolds numbers were possible. In the water experiments, limitations of the cart drive motor permitted testing at  $Re_{\infty}$  of 0.5 to  $1.0 \times 10^4$  per foot. With the wind tunnel experiment,  $Re_{\infty}$  varied from 0.8 to  $1.8 \times 10^5$  per foot. For typical properties of sea water (35% salinity and temperature of  $0^{\circ}\text{C}$ . at a depth of approximately 2000 meters<sup>12</sup>) this Reynolds number range would correspond to a velocity range of 0.1 to 3.0 ft/sec in a deep oceanic vehicle.

Results of the tow tank investigation of  $20^{\circ}$  and  $30^{\circ}$  plate-wedge configurations are contained in Figure 5. In the streak line photographs, the limits of the recirculation eddy are indicated by an "S" and an "R" indicating respectively the points of flow separation and

reattachment. The results of the higher Reynolds number wind tunnel tests are contained in the series of pressure distributions in Figure 6. Static pressures were read with a water-filled micromanometer referenced to atmospheric conditions. On the 20° wedge model, the first, second, and fourth pressure taps were obstructed at the time of testing and thus no readings were obtained at those stations.

All of the pressure surveys exhibit the same basic characteristics. An adverse pressure gradient preceeds separation of the boundary layer; a constant pressure region characterizes the separation itself; the pressure then rises again due to either recompression, transition, or possibly both. Beyond reattachment, the pressure drops rapidly, consistent with the acceleration of the mean flow over the wedge.

In the present study, the Reynolds numbers encompassed two flow regimes; the purely laminar separated flow and the case of transitional separation. The influence of Reynolds number on the location of separation is dependent on the character of the flow, a fact well established for high Mach number cases<sup>10</sup>. For the present experimental study, Figure 7 depicts the relationship between Reynolds number and the location of the separation point. The water tank experiments produced essentially laminar separation conditions whereas in the wind tunnel experiments, all cases examined were of the transitional type\*.

---

\*Laminar separation is that in which the separated shear layer remains entirely laminar. Turbulent separation implies a fully turbulent boundary layer ahead of separation. Transitional separation is that in which transition of the separated shear layer occurs (or begins) after separation and before reattachment.

An increase in  $Re_\infty$  produces a forward movement of  $X_s$  provided the flow remains laminar. When the separated shear layer is transitional (or turbulent) the transport of momentum across the shear layer is greatly increased resulting in a deflation of the separation bubble. Consequently, separation is delayed by a Reynolds number increase for the transitional cases.

The dashed curves in Figure 7, connecting the higher and lower Reynolds number data are purely trend lines based upon the type of  $Re_\infty$  dependence reported in supersonic studies<sup>10</sup>. Figure 8 depicts the dependence of the reattachment point on free stream Reynolds number. There is insufficient data here to conclude the exact shape of the curve connecting the higher and lower Reynolds number data. It appears that wedge angle has little affect on the reattachment location for the transitional type of separation.

## CONCLUSIONS

This paper reports the results of an experimental investigation into low Reynolds number flow over a flat plate-wedge configuration, typical of conditions found on vehicle controls of deep ocean submersible vehicles. Flow separation and alteration of the normal pressure distribution was observed. Both laminar and transitional types of flow separation were observed. The Reynolds number dependence of separation and reattachment locations was found to be generally consistent with findings of supersonic plate-wedge investigations.

## REFERENCES

1. Chapman, D. R., Kuehn, D. M., and Larson, H. K., "Preliminary Report on a Study of Separated Flows in Supersonic and Subsonic Streams", NACA RM A55L14, 1956.
2. Chapman, D. R., Kuehn, D. M., and Larson, H. K., "Investigation of Separated Flows in Supersonic and Subsonic Streams with Emphasis on the Effect of Transition", NACA TN 3869, 1957.
3. Hill, W. G. Jr., "Analysis of Experiments on Hypersonic Flow Separation Ahead of Flaps Using a Simple Flow Model", Grumman Research Dept. Memo RM-383, 1967.
4. Lewis, J. E., Kubota, T., and Lees, L., "Experimental Investigation of Supersonic Laminar, Two-Dimensional Boundary Layer Separation in a Compression Corner with and without Cooling", AIAA Journal, 1968, Vol. 6, No. 1, pp. 7-14.
5. Holden, M. S., "Theoretical and Experimental Studies of Laminar Flow Separation on Flat Plate-Wedge Compression Surfaces in the Hypersonic Strong Interaction Regime", ARL 67-0112, 1967, Aerospace Research Laboratories.
6. Ball, K. O. W., and Korkegi, R. H., "An Investigation of the Effect of Suction on Hypersonic Laminar Boundary-Layer Separation", AIAA Journal, 1968, Vol. 6, No. 2, pp. 239-243.

7. Miller, D. S., Hijman, R., and Childs, M. E., "Mach 8 to 22 Studies of Flow Separations Due to Deflected Control Surfaces", AIAA Journal, 1964, Vol. 2, No. 2, pp. 312-321.
8. Hamilton, H. H., and Dearing, J. D., "Effect of Hinge Line Bleed on Heat Transfer and Pressure Distribution Over a Wedge-Flap Combination at Mach 10.4", NASA TN D-4686, 1968.
9. Harvey, W. D., "Experimental Investigation of Laminar-Flow Separation on a Flat Plate Induced by Deflected Trailing-Edge Flap at Mach 19, NASA TN D-4671, 1968.
10. Johnson, C. B., "Pressure and Flow-Field Study at Mach Number 8 of Flow Separation on a Flat Plate with Deflected Trailing-Edge Flap", NASA TN D-4308, 1968.
11. Campbell, D. R., and Mueller, T. J., "A Numerical and Experimental Investigation of Incompressible Laminar Ramp-Induced Separated Flow", University of Notre Dame, Department of Aerospace Engineering Report UNDAS TN-1068-M1, 1968.
12. Riley, J. P., and Skirrow, G., ed., "The Physical Properties of Sea Water", Chemical Oceanography, Vol. 1, Academic Press, New York, 1965, pp. 73-120.

## FIGURE CAPTIONS

Fig. 1 Schematic of water tow tank facility.

Fig. 2 Tow tank test model (near side plate removed).

Fig. 3 Wind tunnel model (near side plate removed).

Fig. 4 Layout of pressure tap locations.

(a) flat plate

(b) wedge face

Fig. 5 Tow tank streak line photographs.

(a) 20° wedge,  $Re_{\infty} = 5,700/\text{ft}$

(b) 20° wedge,  $Re_{\infty} = 8,600/\text{ft}$

(c) 20° wedge,  $Re_{\infty} = 9,800/\text{ft}$

(d) 30° wedge,  $Re_{\infty} = 4,900/\text{ft}$

(e) 30° wedge,  $Re_{\infty} = 6,100/\text{ft}$

(f) 30° wedge,  $Re_{\infty} = 7,800/\text{ft}$

Fig. 6 Surface pressure coefficient vs. distance from plate leading edge.

(a) 20° wedge,  $Re_{\infty} = 8.81 \times 10^4/\text{ft}$

(b) 20° wedge,  $Re_{\infty} = 1.24 \times 10^5/\text{ft}$

(c) 20° wedge,  $Re_{\infty} = 1.49 \times 10^5/\text{ft}$

(d) 20° wedge,  $Re_{\infty} = 1.74 \times 10^5/\text{ft}$

(e) 30° wedge,  $Re_{\infty} = 8.34 \times 10^4/\text{ft}$

(f)  $30^\circ$  wedge,  $Re_\infty = 1.16 \times 10^5/ft$

(g)  $30^\circ$  wedge,  $Re_\infty = 1.40 \times 10^5/ft$

(h)  $30^\circ$  wedge,  $Re_\infty = 1.80 \times 10^5/ft$

Fig. 7 Influence of Reynolds number on location of flow separation.

Fig. 8 Influence of Reynolds number on location of reattachment point.



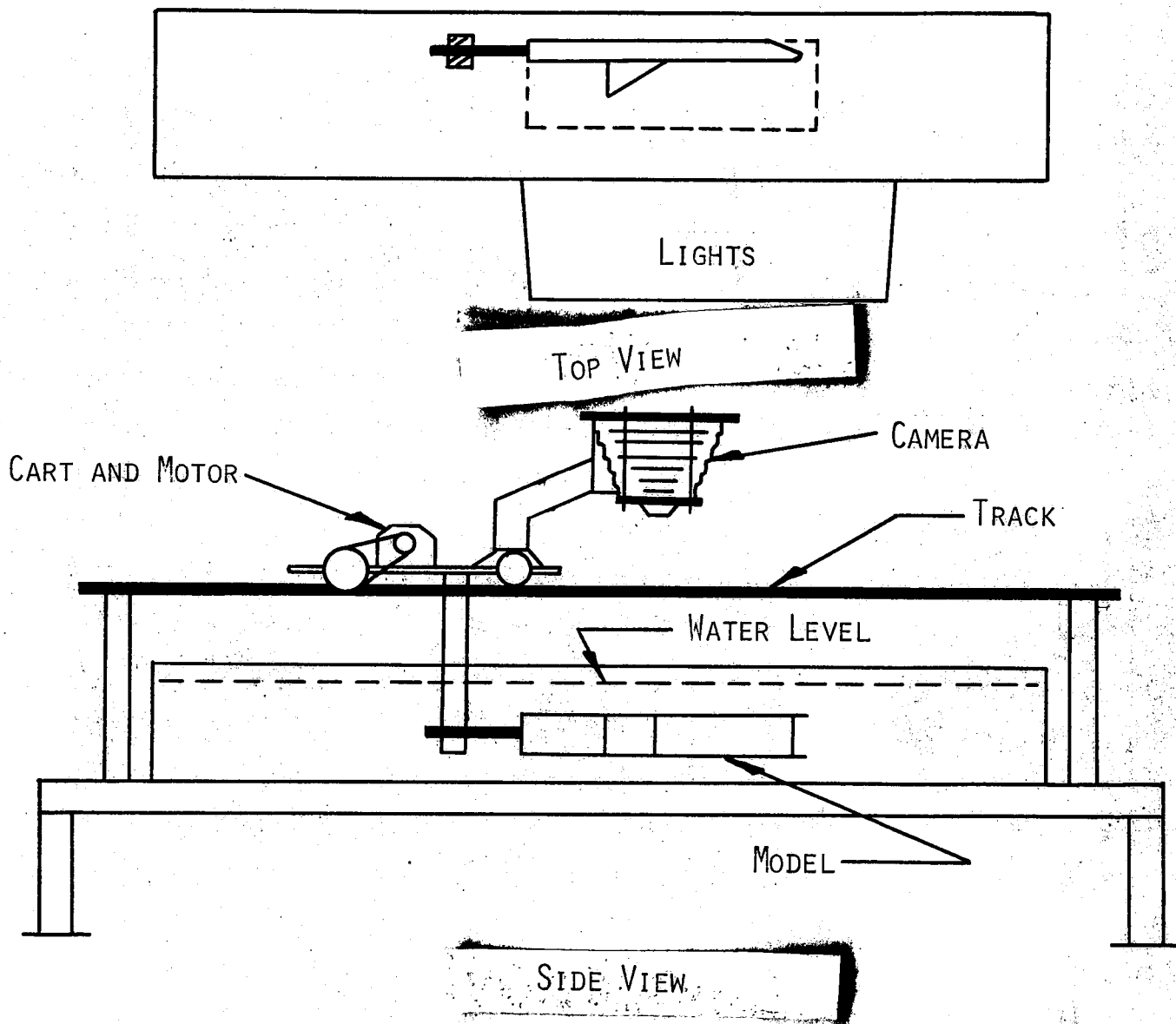


FIGURE 1

Reproduced from  
best available copy.

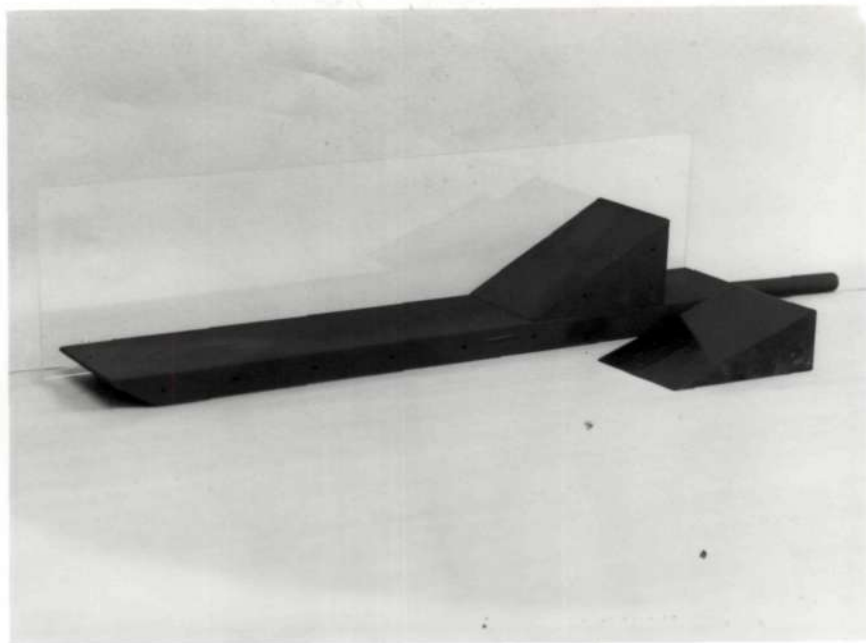


FIGURE 2

Reproduced from  
best available copy.

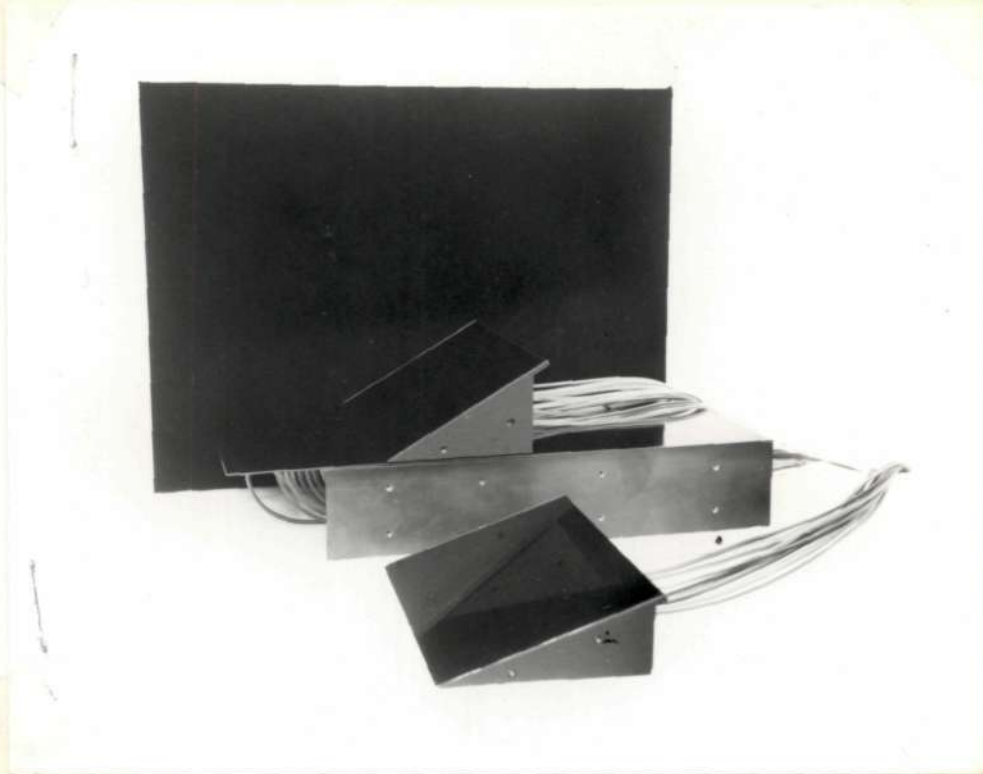


FIGURE 3

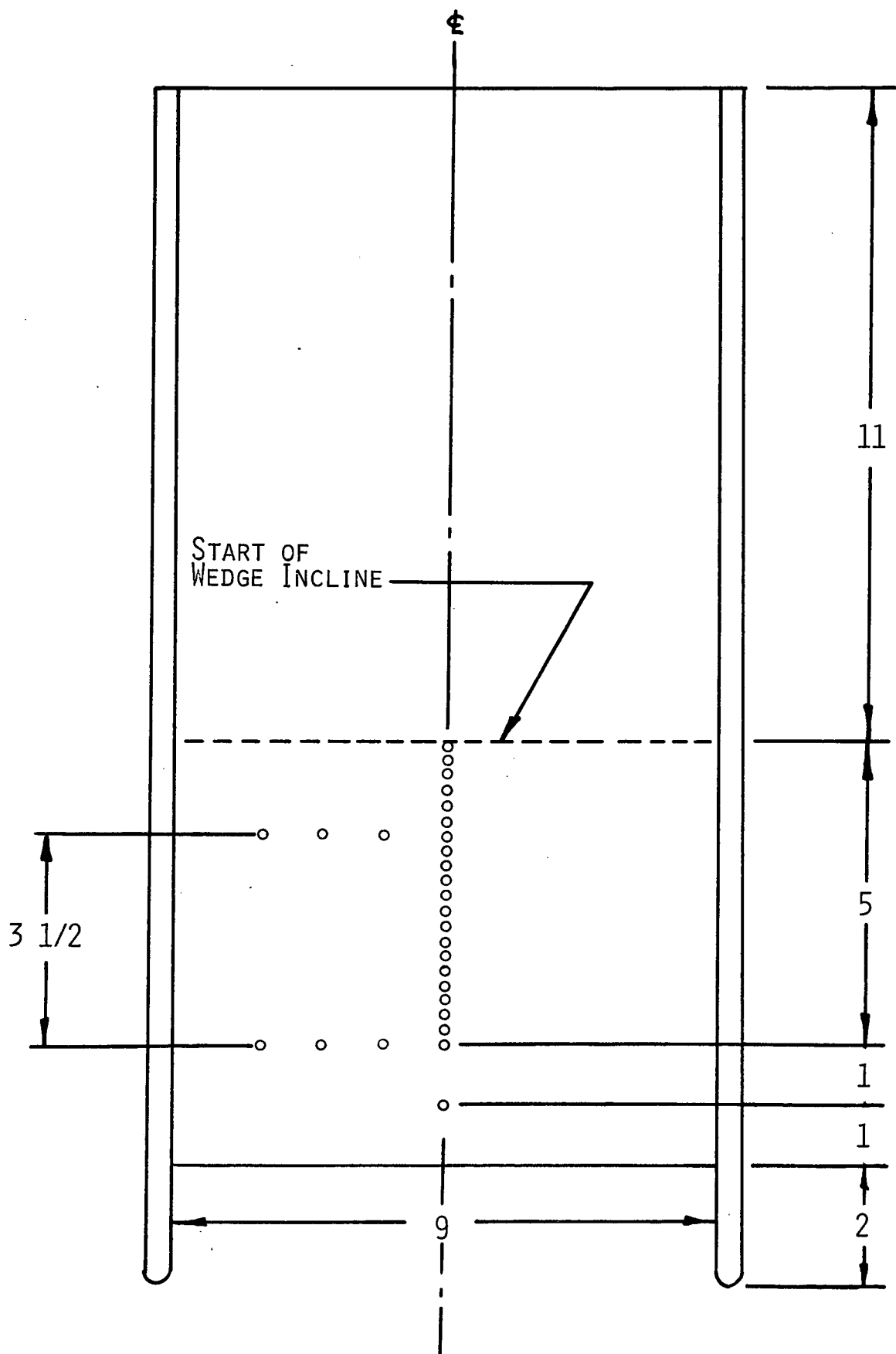


FIGURE 4-a)

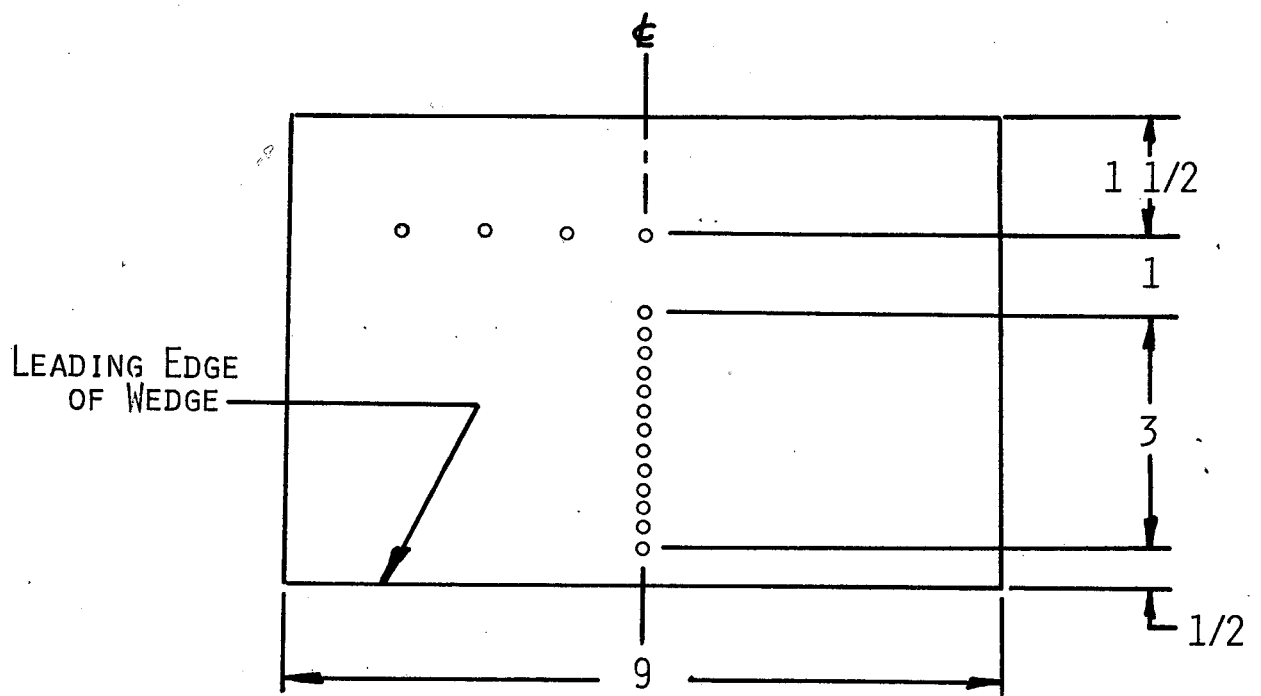
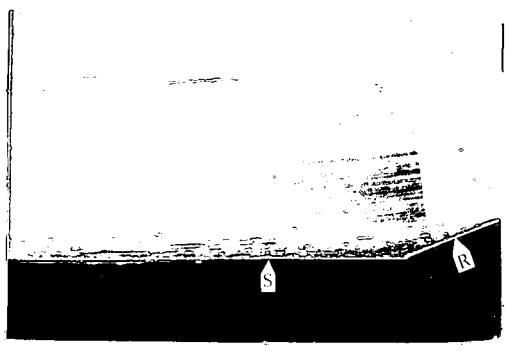
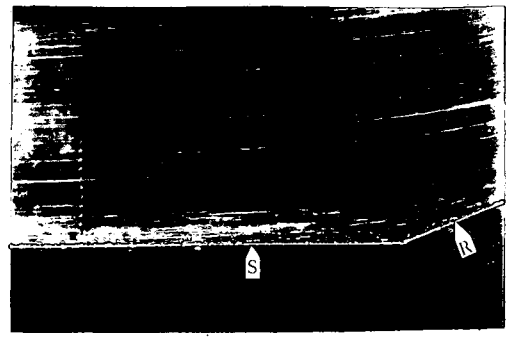


FIGURE 4-b)

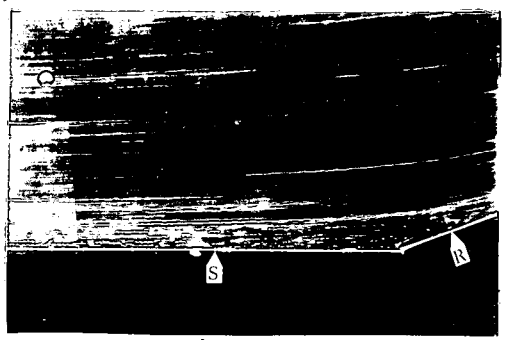
Reproduced from  
best available copy.



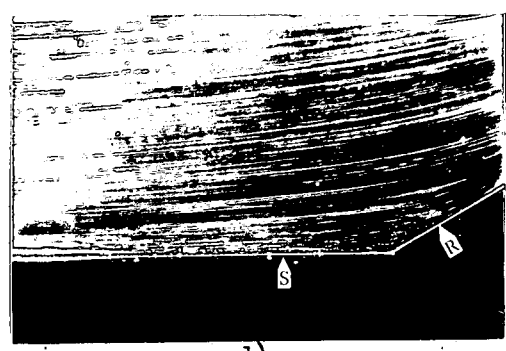
a)



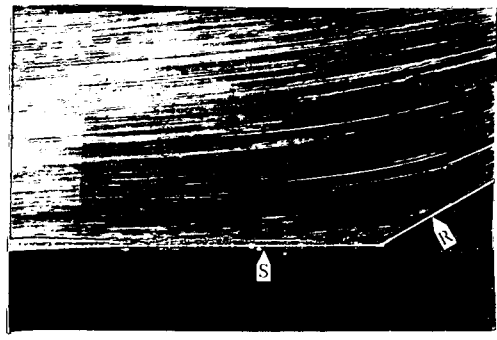
b)



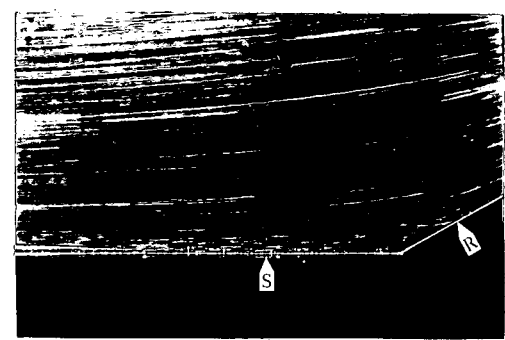
c)



d)



e)



f)

FIGURE 5

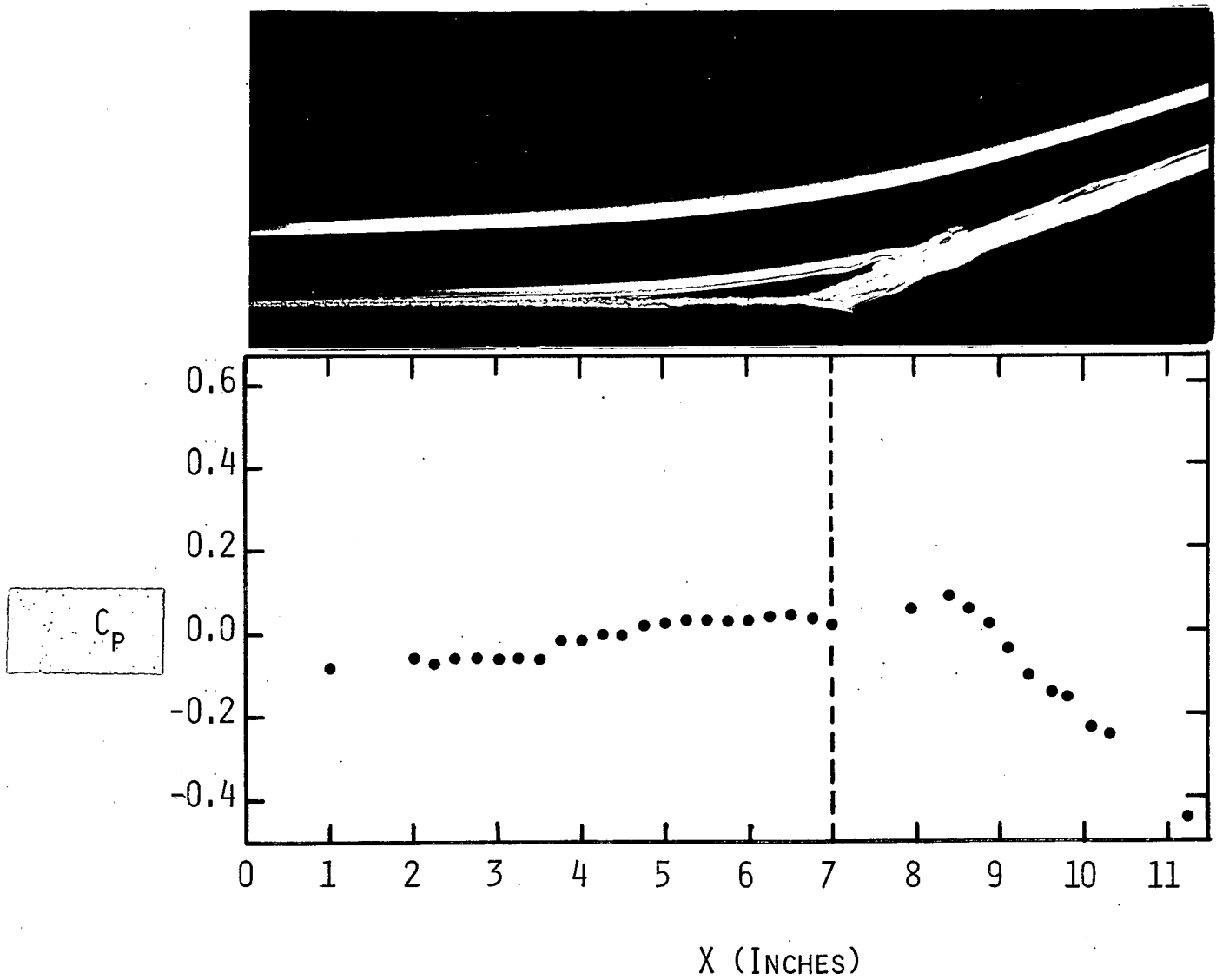
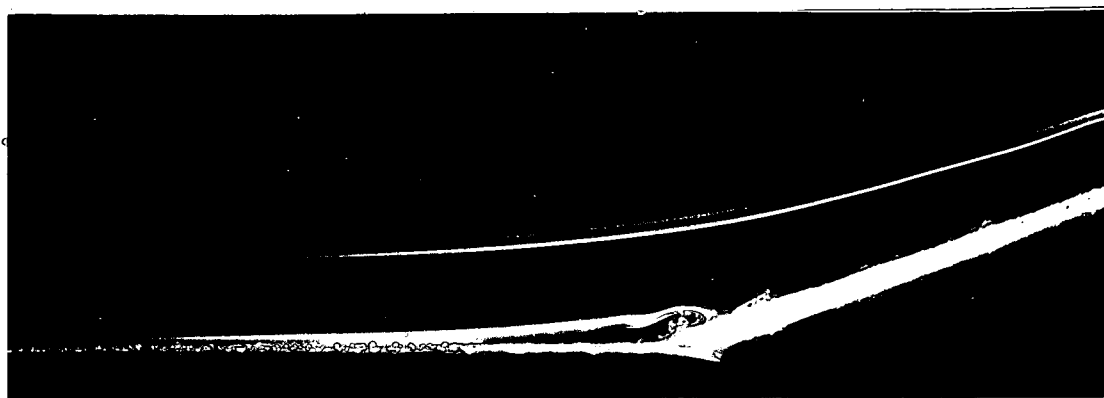
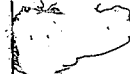
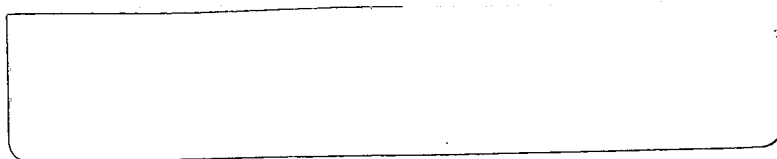


FIGURE 6-a)



$C_P$

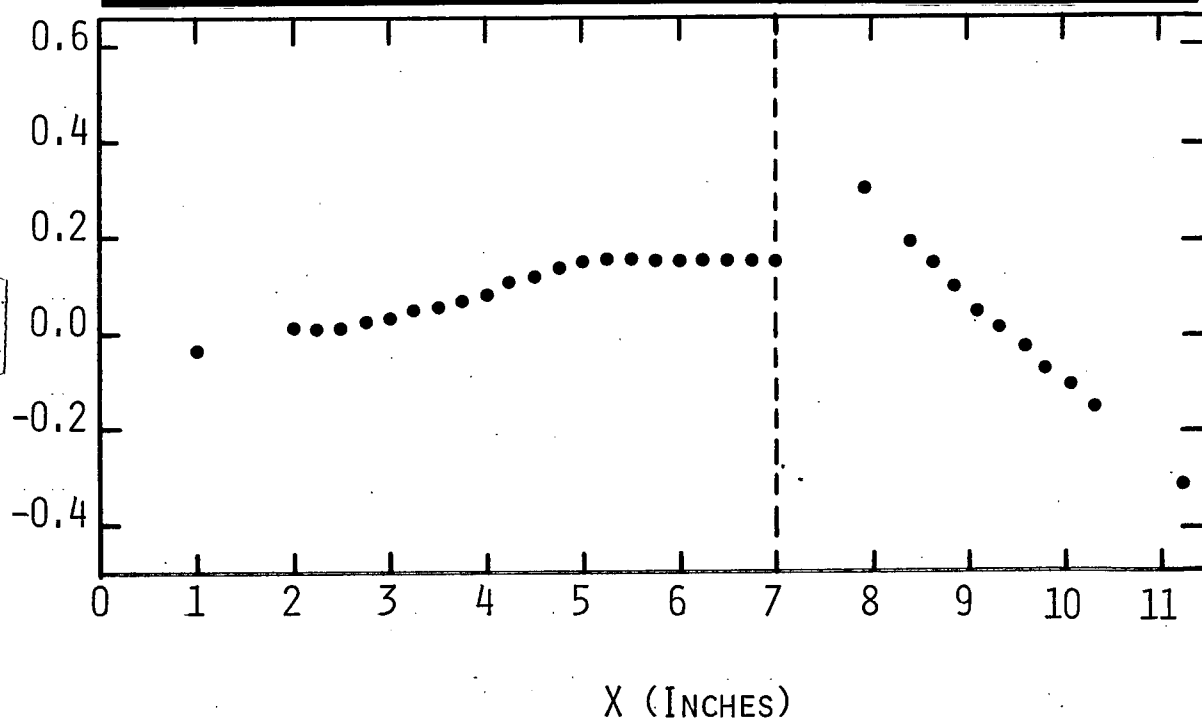


FIGURE 6-b)



Reproduced from  
best available copy.

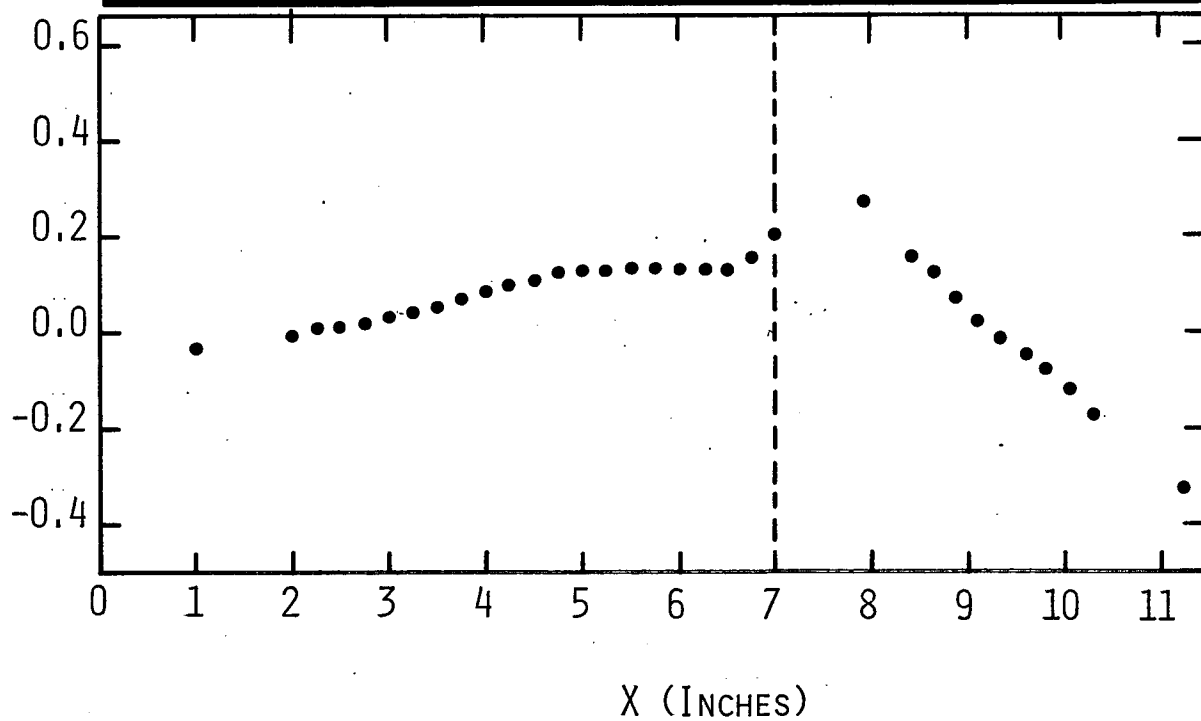


FIGURE 6-c)

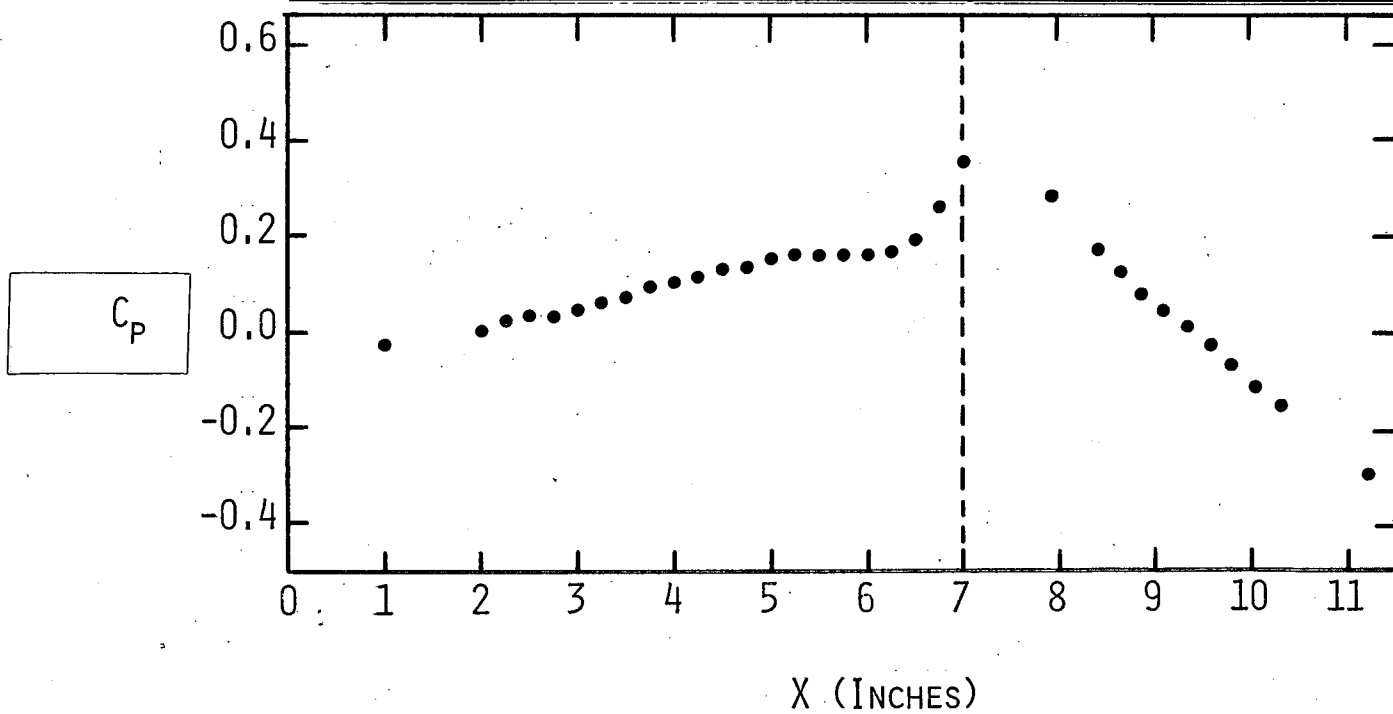
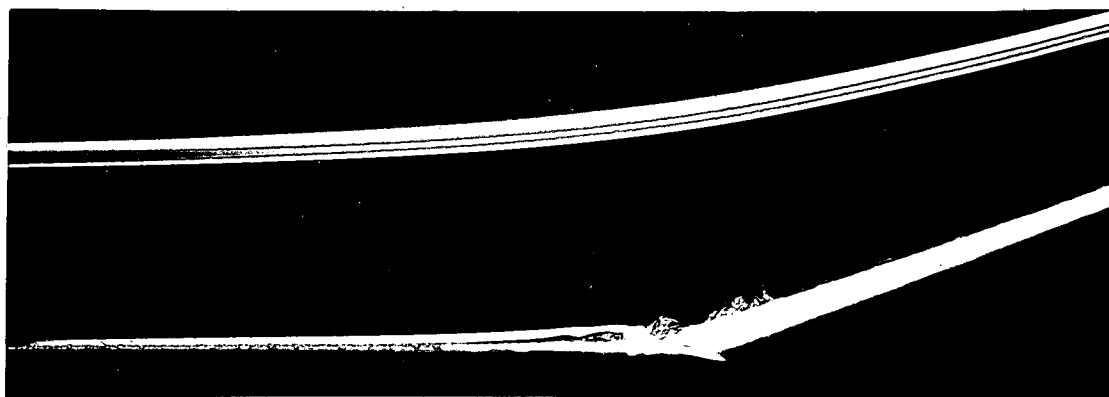
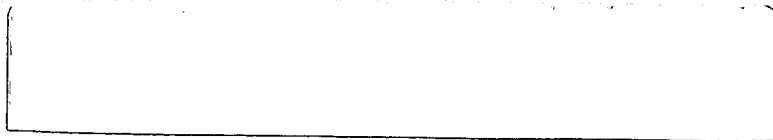


FIGURE 6-d)

Reproduced from  
best available copy.

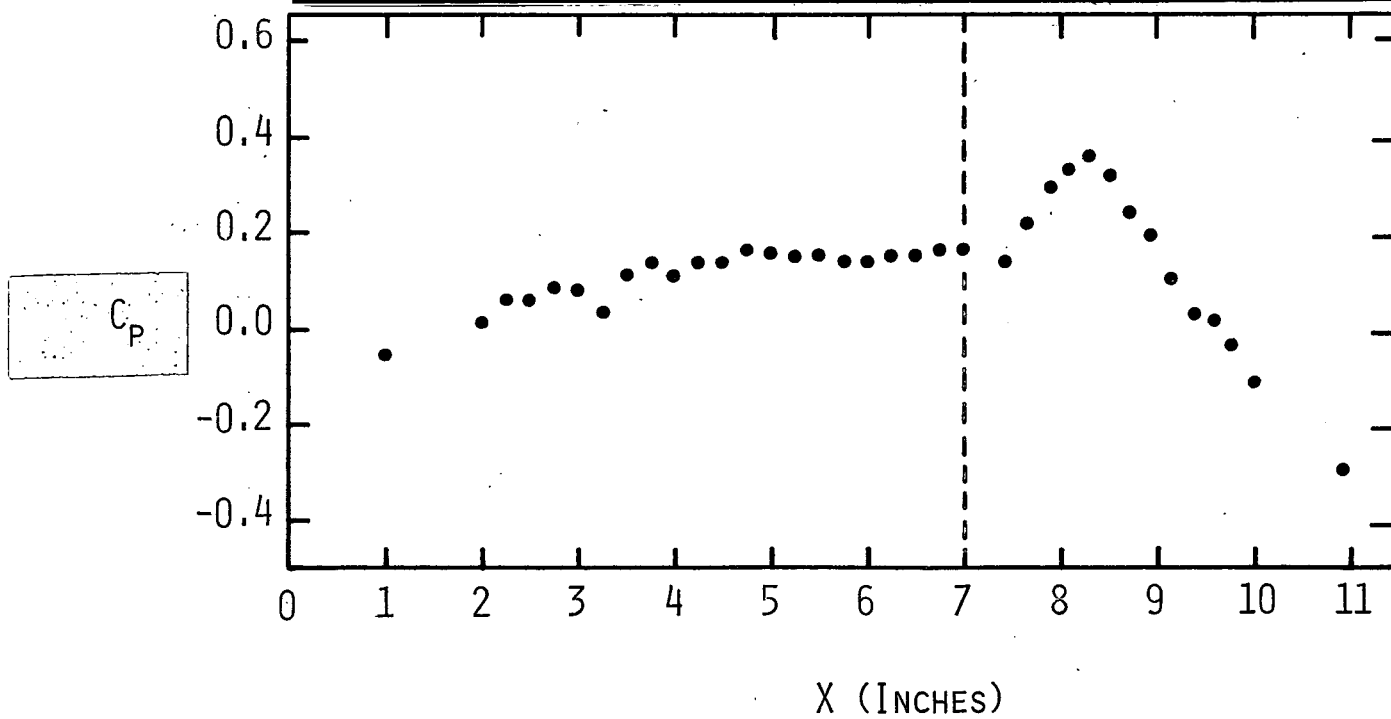


FIGURE 6-e)

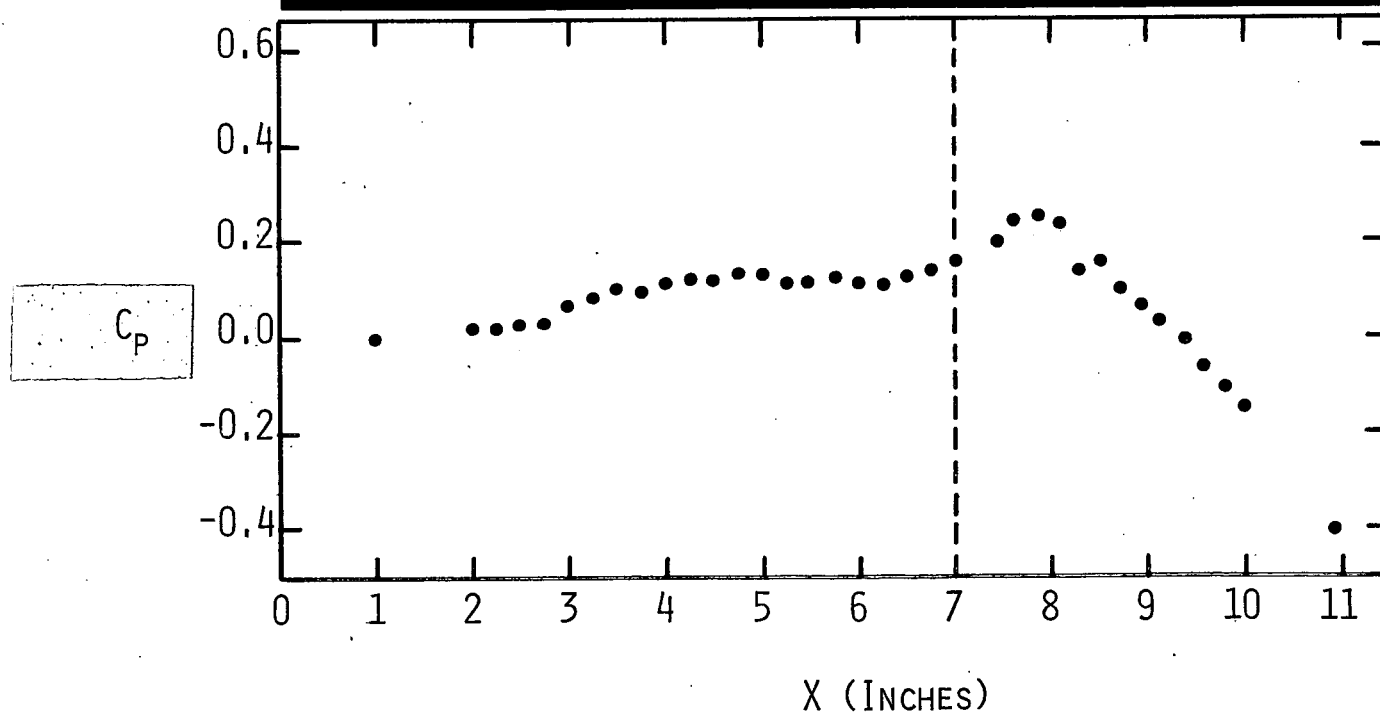
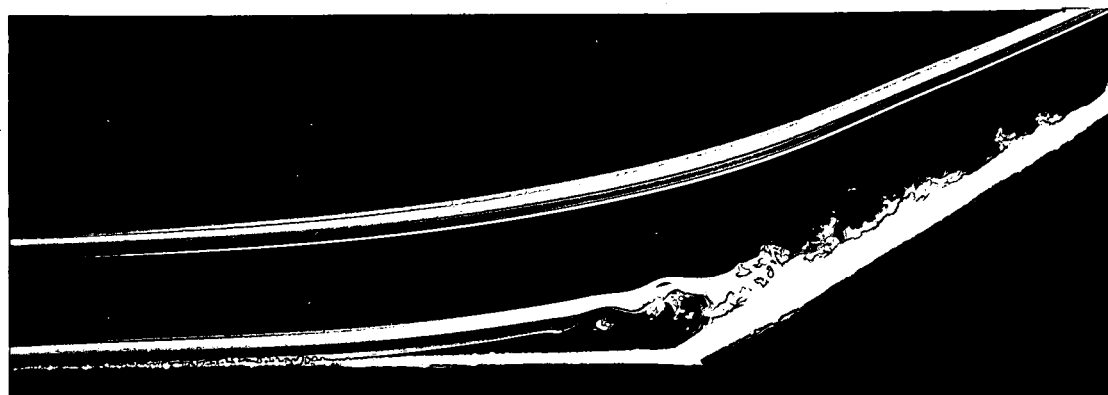
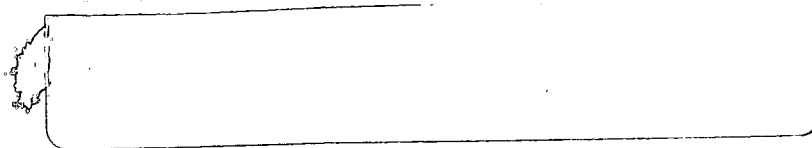


FIGURE 6-f)

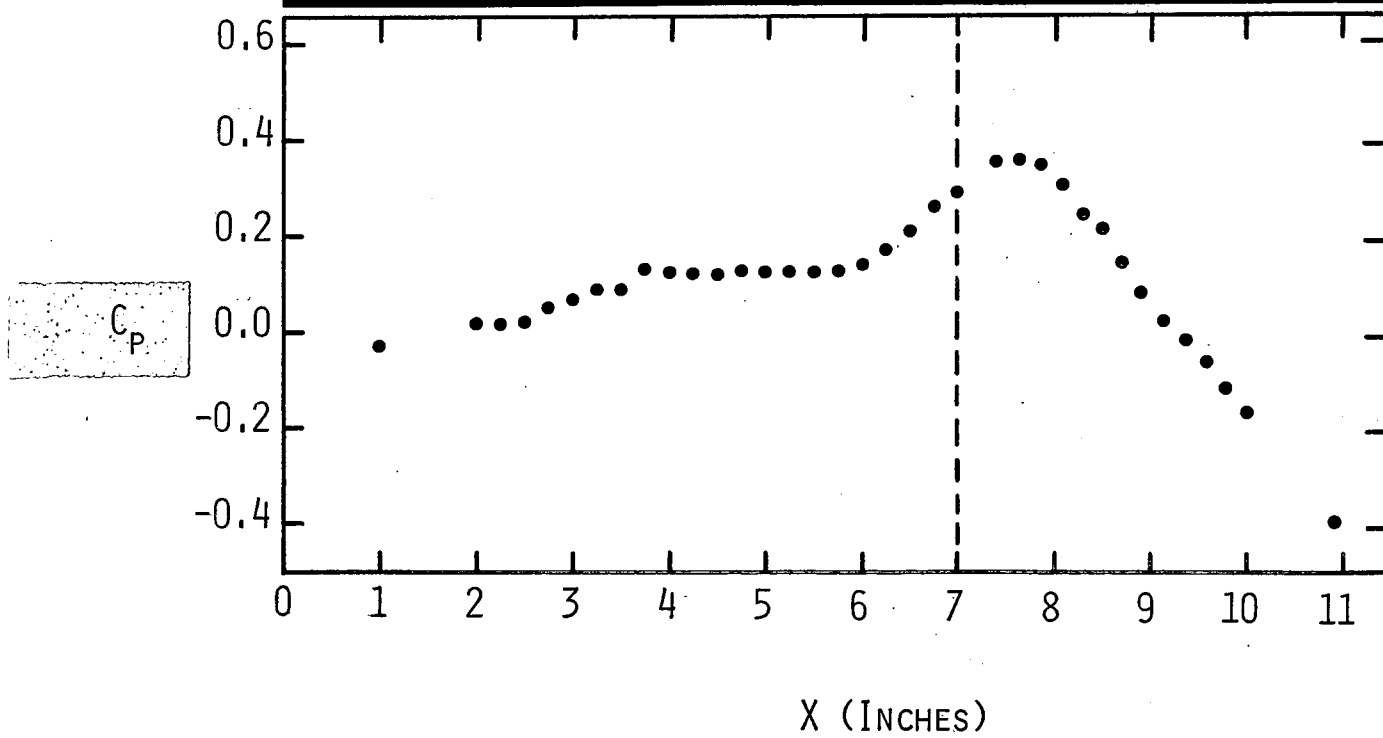
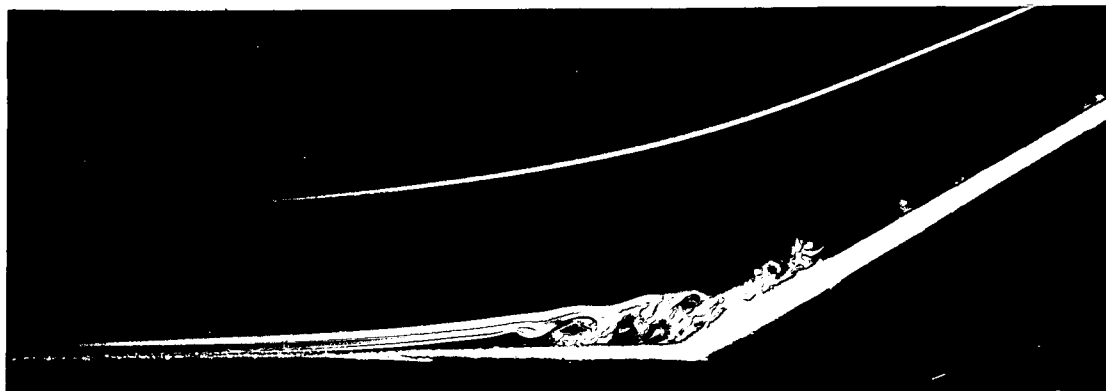


FIGURE 6-g)

Reproduced from  
best available copy.

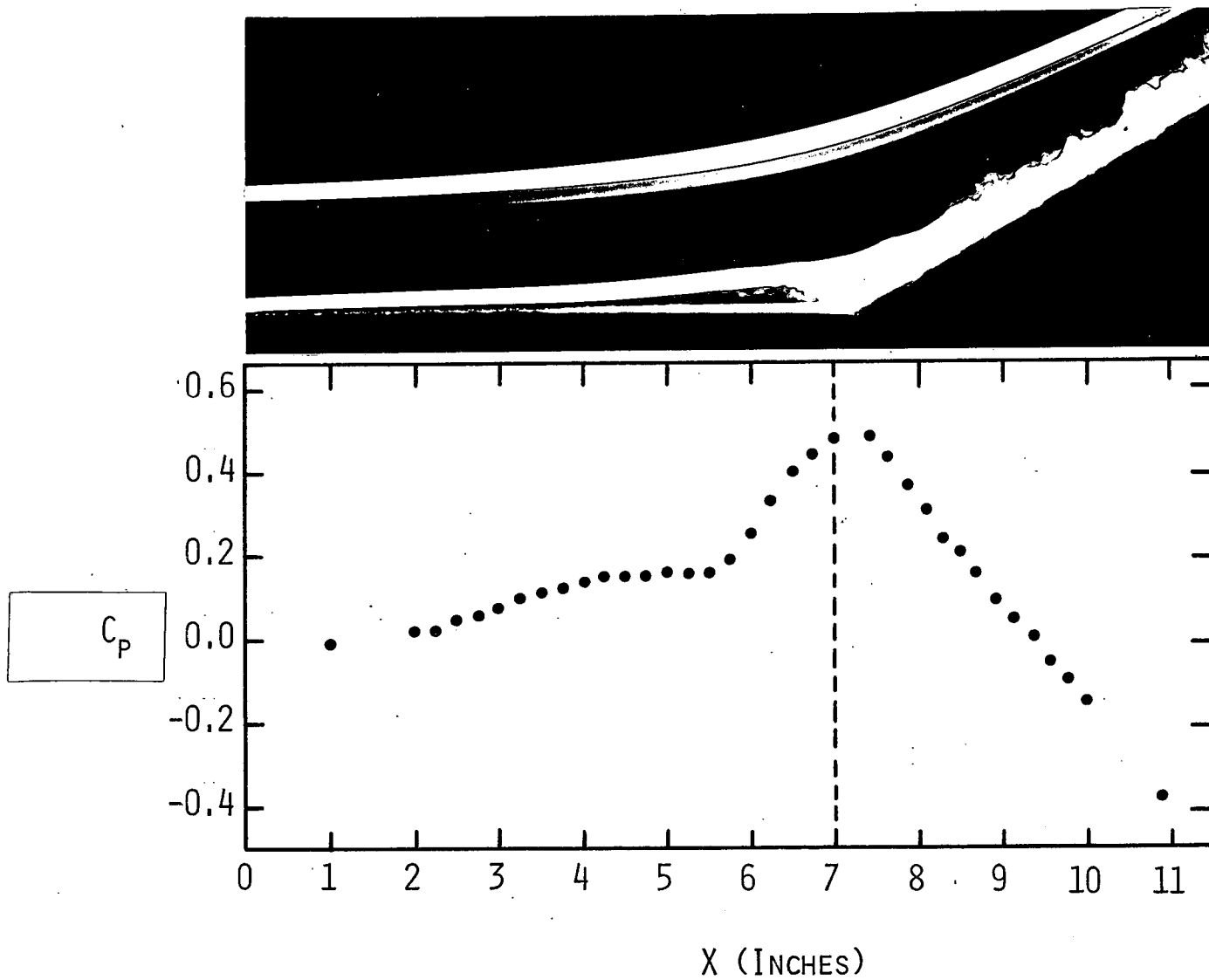


FIGURE 6-h)

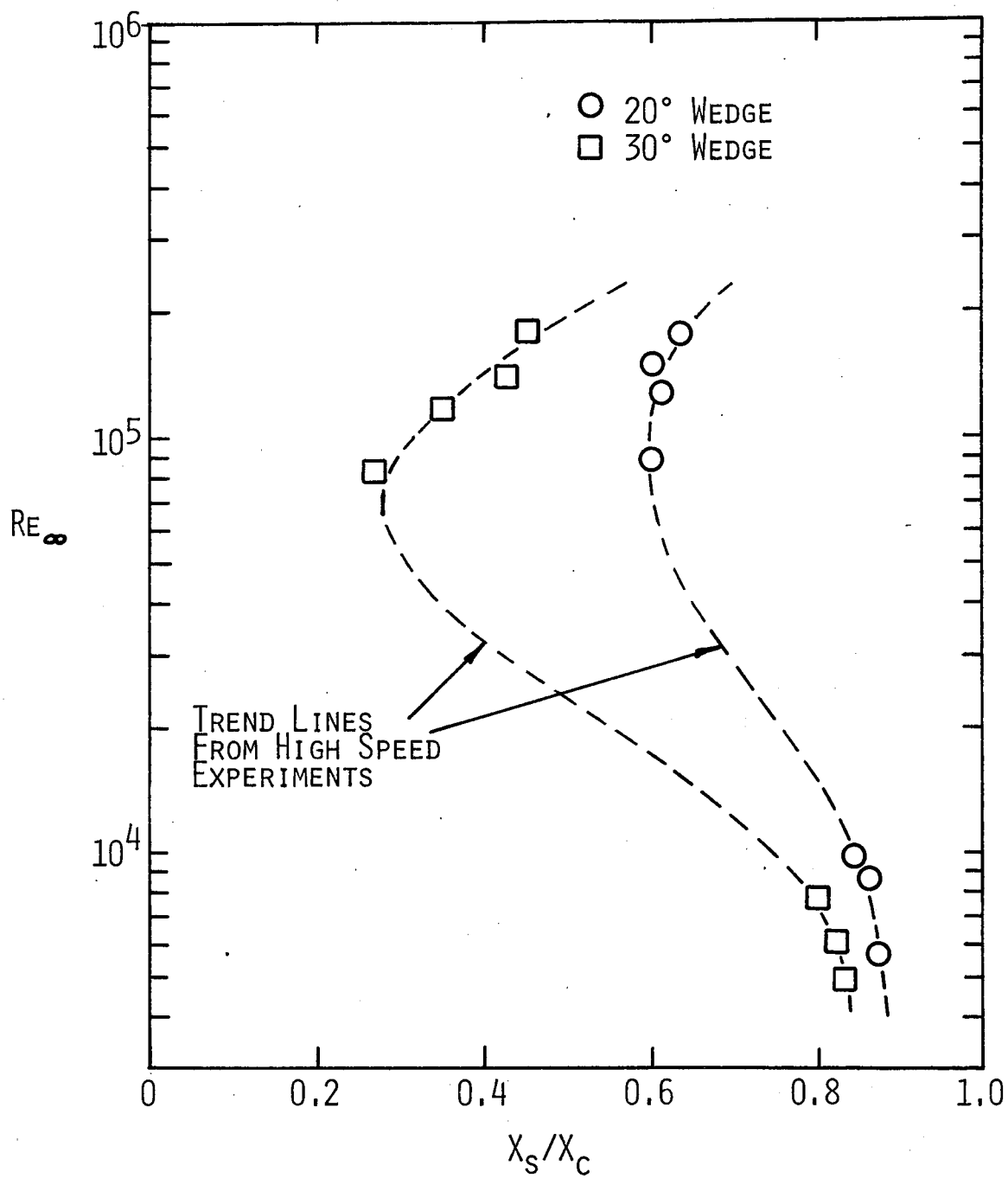


FIGURE 7

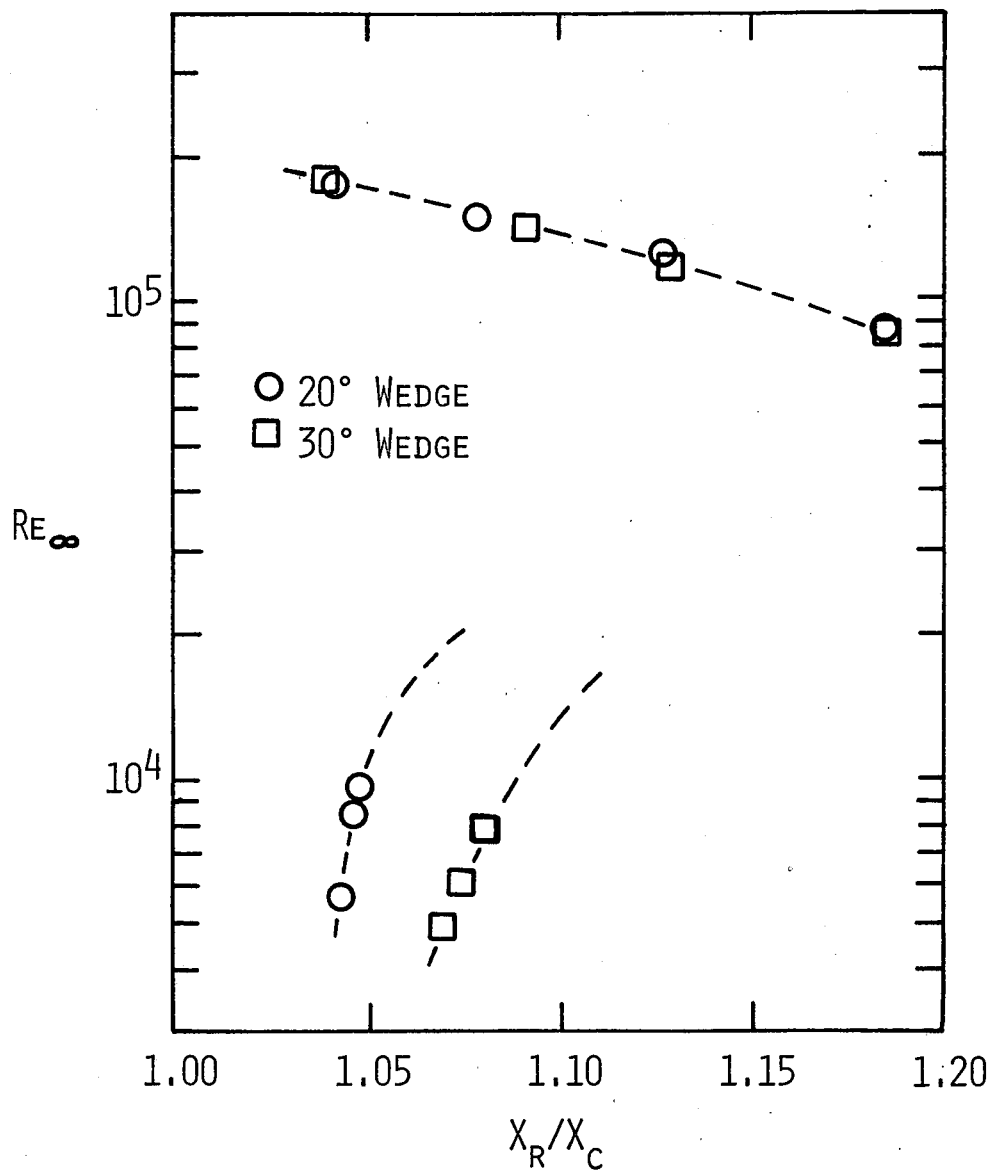


FIGURE 8